Tutor/s

Dr. Irene Garcia Cano
Departament de Ciència dels Materials I Enginyeria Metal·lúrgica.

Dr. Núria Cinca Luis
Centre de Projecció Tèrmica

Grau en Enginyeria Química

Treball Final de Grau

Cold gas-sprayed titanium aluminide coatings: production and characterization.

Recobriments d' aluminur de titani utilitzant la Projecció Freda: producció i caracterització.

Robert Bargués Bermejo

June 2016

Universitat de Barcelona

Dos campus d'excel·lència internacional

B:KC Barcelona Knowledge Campus

HUBc Health Universitat de Barcelona Campus

En lloc de ser un home exitós, busca ser un home valuós, la resta arribarà naturalment.

Albert Einstein

En primer lloc vull agrair als meus pares i al meu germà per ser amb mi tant en els bons com en els mals moments i ajudar me en tot el que poden.

També vull agrair a tots els membres del CPT que m'han permès realitzar aquest treball amb ells. Especialment, a Núria per ajudar me sempre durant tot aquest treball. També vull donar les gràcies a en Kirian, n'Aina, en John i en Marco per l'ajut rebut i per la bona companyia al laboratori.

REPORT

CONTENTS

1. SUMMARY

Commercial titanium alloys, which are used in automotive and aerospace applications, are characterized by a low specific weight, high strength and an excellent corrosion resistance at relatively low temperatures. In some applications, they are exposed to a combination of high temperatures and mechanical loading as well as wear damage. However, the oxidation and abrasive resistance of titanium at high temperatures are rather poor; alloys such as Ti6Al4V have applications which are limited to temperatures below 500ºC; therefore it is of interest to increase their application temperatures. Several methods have been employed to increase the oxidation resistance to 900ºC. Among them, the use of titanium aluminide coatings has been considered of interest, especially the titanium trialuminide, which possesses enough aluminium content to form protective alumina layers. Some approaches to this strategy have included the use of conventional thermal spray technologies. In the present work, we proposed the use of the Cold Gas Spray (CGS) process to first try to form γ-TiAl coatings on Ti6Al4V substrates. Due to some handicaps given by the low deformability of such powder alloy, γ-TiAl+Al composite coatings were produced and annealed afterwards to form the $TiAl_3$. These coatings have been characterized from the microstructural point of view as well as their wear resistance and oxidation performance.

Keywords: Coatings, titanium alloys, intermetallic, oxidation, wear resistance, Cold Gas Spray.

2. RESUM

Els aliatges de titani alumini comercials s'utilitzen en aplicacions de l'industria de l'automòbil y l'industria aeroespacial, es caracteritzen per ser lleugers, tenir una elevada duresa i una elevada resistència a la corrosió a temperatures relativament baixes. En alguns casos, estan exposats a una combinació d'altes temperatures, càrrega mecànica i desgast. Tot i això, la resistència a la oxidació i al desgast del titani a altes temperatures és bastant pobre, els aliatges com el Ti6Al4V tenen aplicacions que estan limitades a temperatures inferiors a 500ºC, per això és interesant incrementar la seva temperatura de treball. S'han utilitzat diferents mètodes per incrementar la resistència a l'oxidació a 900ºC. Per aquestes i altres raons, els recobriments de titani alumini es consideren d'interès, especialment el titani alumini (III) que conté suficient alumini per formar capes protectores d'aluminia. Alguns intents per aconseguir aquest objectiu utilitzen tècniques de projecció tèrmica convencionals. En aquest treball es proposa la utilització de la Projecció Freda (Cold Gas Spray, CGS) per tractar de crear recobriments de γ-TiAl en un substrat de Ti6Al4V. A causa d'algunes deficiències donades per la baixa deformabilitat d'aquest aliatge en pols, es van realitzar recobriments amb composites de γ-TiAl+Al per ser posteriorment tractats tèrmicament i formar $TiAl_3$. Aquests recobriments han sigut caracteritzats des del punt de vista microestructural així com la seva resistència al desgast i a la oxidació.

Paraules clau: Recobriments, aliatges de titani, intermetàl·lics, oxidació, resistència al desgast, Cold Gas Spray

3. INTRODUCTION

The present work is focused on the use of titanium aluminides for wear and oxidation protection of titanium alloy substrates. Titanium aluminides are transition metal intermetallic compounds with potential interest [1]. In comparison to conventional titanium alloys, TiAl- based alloys are the most intensively studied because of their low densities, strength and modulus retention at high temperatures, some tensile ductility at room temperature, and reasonably good oxidation resistance. This makes them very attractive as a new class of light-weight high-temperature materials for structural applications, especially in advanced aerospace engine and airframe components.

3.1. TITANIUM ALUMIDES, SOME CONCEPTS ON STRUCTURE, PROPIERTIES AND APLICATIONS

The interest in titanium aluminide alloys concentrates on alloys on the basis of the TiAl-phase. They are known as γ -TiAl alloys or gamma titanium aluminides and excel by their high specific strength. These alloys contain the α_2 phase (Ti_3Al) as a second phase and are alloyed with further elements for property optimization. These alloys can be produced by both powder metallurgy and ingot metallurgy. They are processed in various ways to produce different microstructures with different property combinations, which can be modified by thermo mechanical treatments.

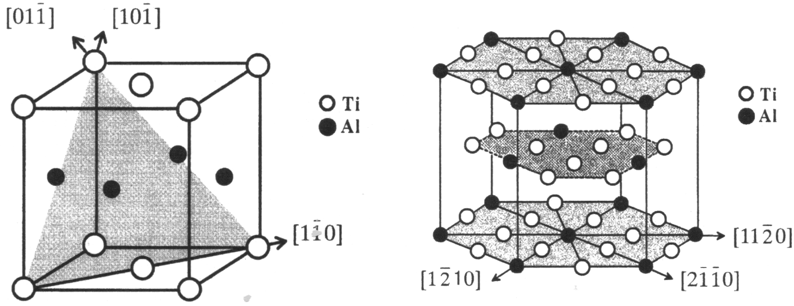

Fig 1: TiAl Crystal structures of the (a) $L1_0$ and (b) $D0_{19}$ types. [2]

Various versions of the binary Ti-Al diagram are available, which are still under discussion because of conflicting results on the various phase equilibrium. The phase diagram in Fig. 2 considers recent results. The alloy developments on the base of the titanium aluminides have made use of alloying with further elements, in particular Nb, V, and Cr [3].

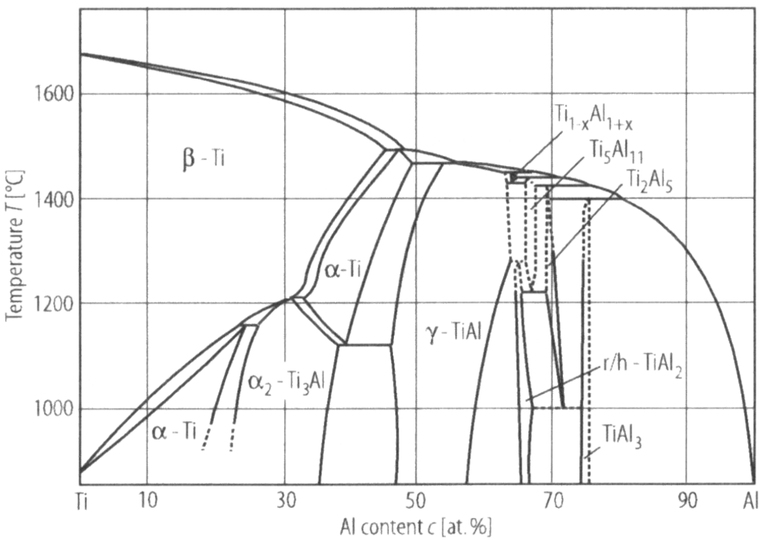

Fig 2: Ti-Al phase diagram [3]

Nowadays, the intermetallic TiAl alloys of actual great engineering interest follow the chemical compositions in the range Ti-(45-48)Al-(1-10)M (at.%), with M being at least one element from V, Cr, Mn, Nb, Ta, W, and Mo [4]. These alloys can be divided into single phase γ(TiAl) and two phase γ(TiAl) + α_2(Ti_3Al) alloys. Single phase γ-alloys contain third alloying elements such as Nb or Ta that promote strengthening and additionally enhance oxidation resistance. The role of the third alloying elements in two phase alloys is to raise ductility (V, Cr, Mn), oxidation resistance (Nb, Ta) or combined properties. Additions such as B and Mg can markedly enhance hot workability, W and C increase creep resistance and, reduction of O enhances room temperature tensile elongation. Depending on chemical composition and heat treatments, TiAl-based alloys exhibit four different types of microstructures: near-gamma, duplex, near lamellar and fully lamellar microstructure (table 1) [4].

Type	**Phase distribution**	**Properties**
Near-gamma (NG)	γ grains + α_2 particles	
Duplex (DP)	γ grains + α_2 plates or particles	Higher tensile strength, ductility and longer fatigue life
Nearly lamellar (NL)	Lamellar γ + γ grains	Better creep resistance, higher fracture toughness and crack propagation resistance than duplex microstructures
Full lamellar (FL)	Lamellar γ + residual γ grains on grain boundary	
Modified NL (MNL)	Lamellar γ + fine γ grains	
Modified FL (MFL)	Lamellar	

Table 1: Standard microestructures of TiAl-base alloys

Titanium aluminides are lightweight, high-strength materials, thought to be capable of operating just below the temperatures where ceramics are commonly used, making them ideal for elevated temperature. Their beneficial attributes are low density, high melting temperature, relatively good high temperature mechanical properties and reasonable environmental resistance. In the industries TiAl alloys can be used in turbine parts, high-pressure compressor, combustor, tubing, …(Fig. 3). They are mostly produced using conventional casting technology and ingot metallurgy, although there are problems with poor workability, as they are difficult to shape by conventional manufacturing methods such as machining, forging, rolling and extrusion, even at elevated temperatures. To avoid these problems net-shape fabrication technologies such as powder metallurgy have been used. These powder techniques can either use aluminide powder or conform the aluminide during sintering by using reactive powder metallurgy techniques [5].

TiAl-base alloys have been developed worldwide and are on the brink of commercialization. A number of components have been identified for application of Ti-Al base alloys and various jet engine and car engine components have been produced successfully using powder metallurgy approaches [3].

In some applications (valves, rotors and exhaust), Ti-based alloys are exposed to a combination of high temperatures and mechanical, e.g. abrasive, loading. However, the oxidation and abrasive resistance of Ti at high temperatures are rather poor [6]. γ-TiAl, $TiAl_3$ and $TiAl_3$ + $TiAl_2$ aluminide coatings may also be used to protect the conventional alloy such as Ti6Al4V substrates from serious oxidation attack [7].

Fig 3: Valve of TiAl.

3.2. INTERMETALLIC TI-AL COATINGS

3.2.1. Thermal spray coating

Thermal spraying is a generic term to describe a group of coating processes involving kinetic and thermal energy. The raw material, usually in powder form, is melted or partially melted and accelerated onto the substrate. Upon impact, the particles solidify and become mechanically anchored to a previous grit-blasted surface. The particle sizes vary depending upon the process, but can cover a range of 1 to 200 microns [8].

The most common classification is that which presents the techniques according to the energy source. Therefore, the energy sources currently in use are:

Combustion: - Detonation of combustion gases, Detonation Gun.

- Flame created by combustion of gases, Flame Spray and High Velocity Oxygen Fuel (HVOF).

Electric energy: - Sustained plasma created by electrical discharge, Plasma Spray.

- Electric arc, Arc Spray.

3.2.2. Aluminizing

Aluminizing is widely used as a coating method for high-temperature alloys because the process is relatively simple and provides reliable properties of the coating layer for oxidation resistance. The pack aluminizing of TiAl produces a $TiAl_3$ coating layer and, due to the sufficient amount of Al in the coating layer, stable Al_2O_3 is formed when exposed to high temperature oxidation atmosphere. However, the $TiAl_3$ coating layer formed on TiAl is quite brittle and has poor cracking resistance under mechanical loading and thermal stresses produced during pack cementation and oxidation. Thus, the embrittlement of the $TiAl_3$ coating layer prohibits further improvement of the oxidation resistance TiAl alloy under thermal cyclic conditions [9]. Therefore, the formation of a $TiAl_3$ layer is of interest but trying to avoid the embritllement as result of the aluminizing.

3.3. PROBLEMS OF THE DIFFERENT METHODS TO OBTAIN COATINGS

Conventional thermal spray processes tend to lead to a non-homogeneous structure with more or less porosity and phase composition distribution depending on the spraying process and parameters. This fact makes, from one hand that regions with different aluminium contents are formed and, from the other hand that the ordered intermetallic phase is not uniformly obtained along the coating. Such aspects can affect to the desired properties for which material scientists have focused their interest on such compounds since the occurrence of Al-depleted areas can still provide paths for oxygen diffusion [10].

3.4. COLD GAS SPRAY (CGS)

Cold Gas Spray (CGS) is a solid-state spraying technique that produces coatings by exposing a powder, with a certain size distribution, to high-pressure gas stream (nitrogen or helium). These particles acquire high kinetic energy, thus allowing them to reach speeds between 300 and 1200 m/s, depending on several parameters, namely pressure and temperature of the streaming gas, powder composition, particle size and morphology.

There is a basic difference between conventional thermal spray techniques and CGS. While the first technologies require high thermal and kinetic energy to form the coating, in the case of CGS, kinetic energy acquires a major role in the process. The mechanism on how the particles adhere is based on high kinetic energy, localized plastic deformation of impinging particles and substrate (depending on its properties), and adiabatic shear instabilities. In Fig. 5 as shown a schematic view of Cold Gas Spray system.

In Fig. 4 a comparison of particle velocity vs gas temperature for the different spray techniques is shown, where it can be seen that CGS obtains higher velocities at lower temperatures.

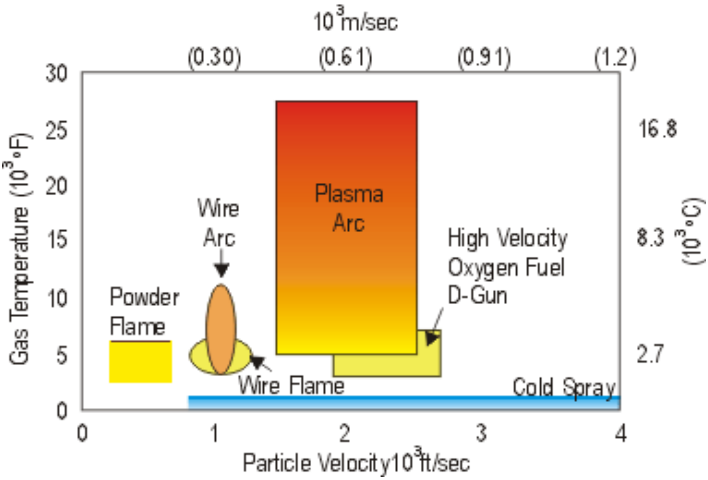

Fig 4: Comparison of the processing temperatures and material transport velocities for the various thermal spray technologies [11]

CGS allows material cost reduction, minimization of surface treatments, possibility of increasing machinery lifetime, and reduction of problems associated with material melting. These features make it an efficient, environmental friendly and economically more affordable than conventional thermal spray and deposition processes [12].

The main advantages that the process involves are:

- Reduction of the porosity of the coating.
- High deposition efficiency, with the possibility of obtaining coating with high density and hardness.
- Reduction of oxides in the coating.
- The composition and microstructure of the starting materials is retained.
- Minimum substrate preparation.
- Possibility of obtaining coatings with high electrical or thermal conductivity.
- Possibility of spraying heat sensitive materials.
- Possibilities reuse the particles, which are not adhered to substrate (100% recycling).
- Operational safety increased due to the absence of a high temperature gas beam, combustion, radiation or explosive gases.

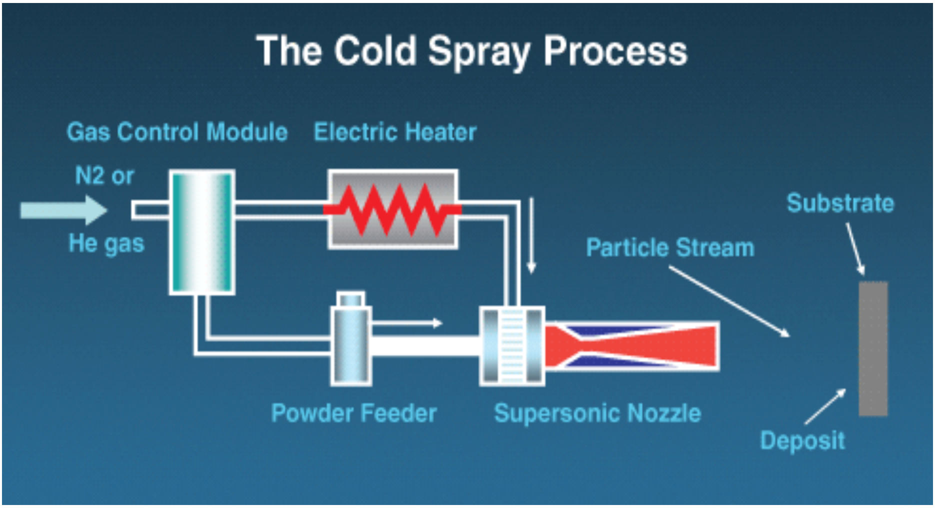

Fig 5: Cold Gas Spray system

4. Objectives

The main aim of this work is to obtain intermetallic Ti Al + Al coating using Cold Gas Spray to achieve high temperature and wear resistance, which might be applied to the automobile and aerospace industry. To achieve that, some specific objectives need to be considered:

- Obtain intermetallic Titanium aluminide intermetallic coatings using Cold Gas Spray.
- Study of the coating deposition.
- Achieve Ti Al_3 coating using different heat treatments.
- Microstructural, wear and oxidation characterization.

5. EXPERIMENTAL

5.1. MATERIAL AND EQUIPMENT

5.1.1. Material

- **Ti Al powder:** provided by TLS Technik GmbH & Co. Spezialpulver KG, with a nominal composition of Ti48Al2Cr2Nb (at%). Two-phase, near γ-TiAl such as Ti48Al2Cr2Nb have actually been considered for high-temperature structural applications in the aerospace and automotive industries due to their high strength and good oxidation resistance at elevated temperatures [13]. Oxidation resistance is very dependent on small changes of the Al content; for binary alloys, a reduction in Al content from 50 to 48 at% results in increasing the oxidation rate at 900ºC by a factor of four. Of the most commonly used alloying elements, Nb is the most important element to provide TiAl-based alloys with good oxidation resistance. TiAl-based alloys containing Nb, in particular those containing Nb as high as 10at%, whose microstructure can be still in the fully lamellar form, suppress rutile growth and form a thick continuous outer Al_2O_3 scale [2].

- **Al powder**: provided by TLS Technik GmbH & Co. Spezialpulver KG, with a purity of 99,7%. A blend of TiAl-Al composite was employed with two purposes: first because a better deposition can be achieved due to the ductility of the aluminum powder behaving as the ductile matrix for proper spraying of the harder and more brittle TiAl particles and, second with the aim to posteriorly obtain $TiAl_3$.

5.1.2. Equipment

5.1.2.1. Sample preparation

- **Vibrating Sifter:** along with Retsch sieves with mesh size of 24 and 60 μm allow separate the powder depending of the particle size.

- **Furnace:** The Carbolite tubular furnace allows work with different atmospheres.
- **Hot mounting Press:** The sample with the Bakelite (Struers) is introduced into the Hot mounting press. By applying pressure 20 KN and temperature of 180ºC during 5 minutes is melting the Bakelite. After cooling time 3 minutes, the sample is stuffed.
- **Grinding and polishing machine:** Used for metallographic preparation, the grinding is done with SiC papers, existing different grain sizes between grit 80 to 4000. The final polishing is done using lubricant and a diamond suspension with particle size of 1 and 6 μ m.

5.1.2.2. Sample characterization

- **Optical microscope:** Leica DMI5000 M. Allows take images of the different samples. Imaging can be performed at different magnifications since 100x to 1000x.
- **Nano indentation:** The material hardness and stiffness has been calculated automatically by using a nanoindentation Nano Indenter® XP system (Systems Corporation) equipped with Test Works 4 Professional level software. Connected at an optical microscopy allows to select the area that we want to know the hardness.
- **Scanning Electron Microscopy (SEM):** for the microstructural observation, also a Scanning Electron Microscope (JEOL 5310 microscope) was used. It uses a focused beam of high-energy electrons to generate a variety of signals at the surface of solid specimens. The signals that derive from electron-sample interactions reveal information about the sample including external morphology, chemical composition, and crystalline structure and orientation of materials making up the sample. In most applications, data are collected over a selected area of the surface of the sample, and 2-dimensional image is generated that displays spatial variations in these properties. Areas ranging from approximately 1 cm to 5 microns in width can be images in a scanning mode using conventional SEM techniques (magnification ranging from 20x to approximately 30.000x, spatial resolution of 500 to 100 mn).
- **X-Ray Diffraction (XRD):** for the phase analysis, a X-ray diffraction (Bragg Brentano $\theta/2\theta$ Siemens D-500 diffractometer with Cu Kα radiation) was used. It relies on the dual wave/particle natures of X-rays to obtain information about the structure of crystalline materials. A primary use of the technique is the identification and characterization of compounds based on their diffraction pattern.

The dominant effect that occurs when an incident bean of monochromatic X-rays interacts with target material is scattering of those X-rays form atoms within the target material. In materials with regular structure, the scattered X-ray undergoes constructive and destructive interference. This is the process of diffraction. The diffraction is described by Bragg's Law $n\lambda = 2d \cdot sen\,(\theta)$. The directions of possible diffractions depend on the size and shape of the unit cell of the material. The intensities of the diffracted waves depend on the kind and arrangement of the atoms in the crystal structure. [14]

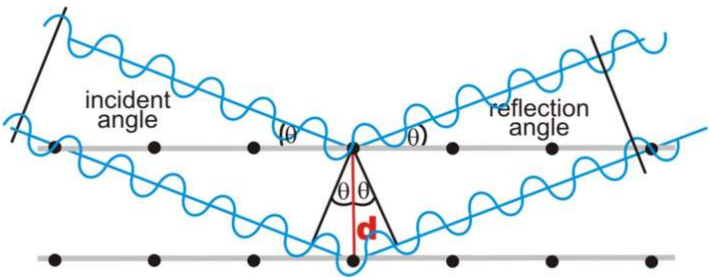

Fig.5: Representation of Bragg's Law [15]

- **Ball on Disk**: Used to calculate easily the coefficient of friction and evaluate the dry sliding wear behavior. For this evaluation, a Ball-on disc test (ASTM G99-03) has been performed and the wear rates were calculated from the Δvolume in the wear track by means of confocal microscopy.

5.2. EXPERIMENTAL PROCEDURE

Scanning Electron Microscopy and optical microscopy were mainly used to examine the supplied material as well as to characterize the impact morphologies and coating formation. Additionally, a heat treatment at 1440ºC with Argon for 20 minutes, heating rate 5ºC/min was performed to the as-supplied powder to induce the formation of a microstructure other than the as-supplied one [16].

The Ti6Al4V substrates were mirror-like polished and cleaned in an ultrasonic bath prior to the cold spraying of the Ti-48Al-2Nb-2Cr powder. Wipe tests were performed on the mentioned substrates in order to observe the feasibility of plastic deformation of single particles, which gives an idea of their suitability prior to coating formation when using a specific set of spraying conditions.

The spraying was performed with a KINETICS® 4000 equipment with N_2 as the propelling gas. Different spraying conditions were primary tested with the aim to evaluate not only their influence but also the influence of the substrate material.

Sample Name	Temperature (ºC)	Heating rate (ºC/min)	Atmosphere	Time (h)
1	-	-	-	-
2	500	3	Ar	5
3	600	3	Ar	5
4	650	3	Ar	5
5	700	3	Ar	-
6	700	3	Ar	1
7	700	3	Ar	1,5
8	700	3	Ar	5

Table 2: Representation of different annealing treatment.

The Ti-48Al-2Nb-2Cr powder was afterwards blended with pure Aluminium in the right proportion to form $TiAl_3$.

The TiAl+Al composite CGS coatings were then exposed to different annealing treatments under argon atmosphere in a tubular furnace in order to assess the formation of the $TiAl_3$ phase. The annealing treatments conditions were shown in Table 2. All the samples were heated and cooled at an average rate of 3ºC/min.

The cold gas sprayed coatings were mounted in a conductive resin and afterwards ground and polished for the inspection of the cross section. X-ray diffraction was used to evaluate the phase composition and a nanoindentater was employed to obtain the hardness and young modulus of powder and coating systems.

Finally, the wear testing was evaluated for the original Ti6Al4V substrate and compared with the as-sprayed TiAl+Al and annealed coating. The Ball-on disc test has allowed the examination of the friction coefficient of the polished coating materials and the wear track was examined by means of confocal microscopy. The examination of the damaged surfaces determines the wear mechanism. These tests were carried out with 14 mm diameter WC-6Co ball that was frictioning the polished coating surface (below 0.8 Ra). A temperature around 25 ºC and the humidity (below 20%) were controlled during the test time into the closed camera where the experiments were performed. A sliding speed of 0,11 m/s, track diameter of 16 mm and sliding distance of 1000 m were constant for all the tests.

The isothermal oxidation test was performed in atmosphere of Oxygen at 750 and 900ºC for 24 hours in a Hobersal CR 32 furnace under air atmosphere.

6. RESULTS AND DISCUSION

6.1. TIAL (TI48AL2NB2CR)

6.1.1. Powder characterization

6.1.1.1. Particle size

In the Cold Spray, the particle size is a critical parameter. Usually, particle size distributions between 10-50 microns are used. A narrow particle size distribution will make a powder more suitable for Cold Spray since the particle velocity velocities will be of the same order and, therefore, increased deposition efficiencies can be achieved.

In general, smaller particle sizes have, in average, higher particle velocities. This is because the acceleration of the gas to the particles is inversely proportional to the particle diameter. Actually, the most important parameter in the CGS is the particle velocity prior to impact on substrate. For a given material, exist a critical particle velocity; only the particles reaching a speed over the critical particle velocity can be deposited to produce a coating [17]. The particle velocity is directly related to the particle size. If available wide range of particle size, the velocity

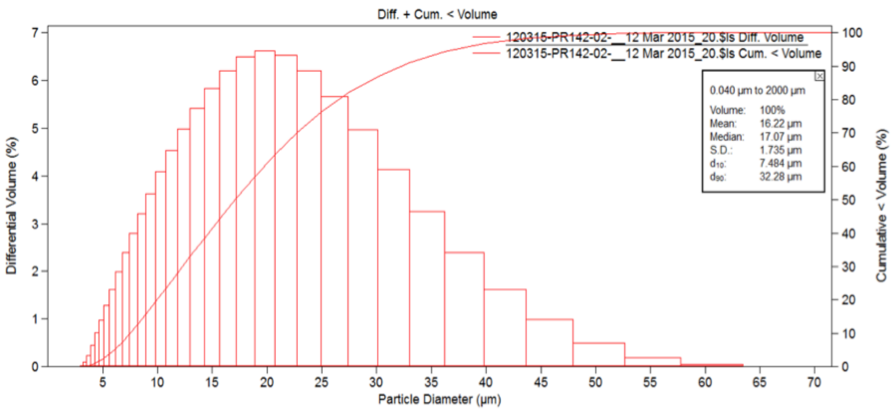

Fig. 6: Particle size distribution

range will be obtained also wide, since it has been commented previously only the particles reaching a speed over the critical particle velocity can be deposited to produce a coating, so the efficacy is reduced. The particle size distribution of the supplied TiAl powder is shown in Fig. 6. The value of d_{10} = 7,484 μm indicates that 10% in volume of the powder has a size below 7,484 μm, while the d_{90}= 32.28 μm indicates that 90% is below this value; the median size of particle is 17,07 μm. The powder was sieved to eliminate the fraction of particles smaller than 20 μm.

6.1.1.2. SEM and OM

In thermal spray, the powder can be manufactured by different routes and different morphologies are obtained. For the CGS most works use spherical particles to assure that upon impact the stress distribution is as homogeneous as possible.

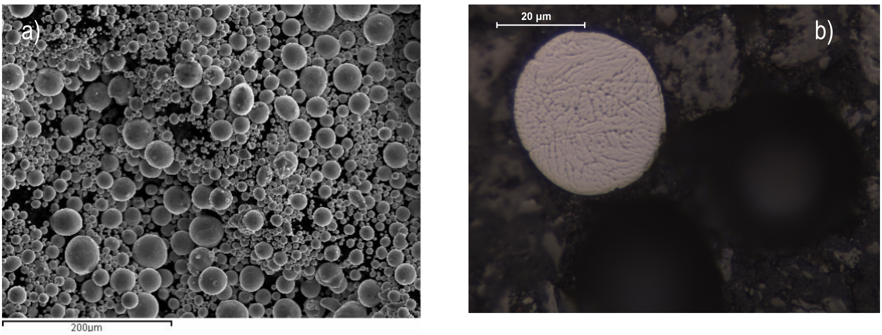

Fig. 7: (a) SEM and (b) OM micrograph of TiAl powder

The spherical particle morphology of the powder is shown in Fig. 7a. It is possible to observe a dendritic structure due to the Gas atomization process (Fig. 7b). During the gas atomization process, the molten metal is atomized thanks to inert gas jets into fine metal droplets, which cool down during their fall in the atomizing tower [18].

6.1.1.3. Nano indentation

The values of Young's modulus obtained for the TiAl (Ti48Al2Cr2Nb) powder are: 131 ± 19 GPa. And the values of hardness obtained are: 6,3 ± 1,6 GPa. The value of Young's modulus is below that the value that shows the literature that is between 160-180 GPa [3]; some differences may be due to the measurement.

6.1.2. Splats

For CGS a minimum of plastic deformation is required; the particles must be deformed to be able to adhere to the substrate and to the rest of particles of the coating.

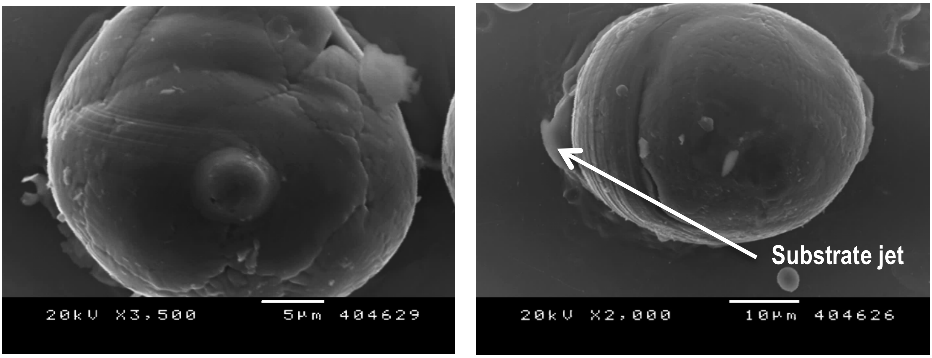

Fig. 8: Two examples of splats of TiAl particles sprayed onto mirror polished Ti6Al4V substrate.

Figure 8 shows the morphology of single deposited Ti48Al2Cr2Nb particles. It is observed that they still keep a spherical morphology, resulting in a low deformation. Because of the higher hardness of the particles compared to the substrate, upon impact, the kinetic energy is more transformed to plastic deformation of the substrate rather than the powder. The particles actually slightly penetrate into the substrate, producing some visible jets. The formation of mutual jets in the particle and substrate is considered to be the optimal for a good bonding [17].

With the aim to try to change the dendritic microstructure and reduce the hardness of the particles, the powder was introduced into a tubular furnace, for an annealing treatment at 1440ºC with Argon for 20 minutes, heating rate 5ºC/min [16]. Yamaguchi et al. [2] reported that fine and homogeneous duplex structures result in good ductility while lamellar structures are poor in ductility. A portion of the resultant bulk was introduced in a zirconia vessel (suitable for the planetary ball mill) the vessel was filled by different diameter zirconia balls. The planetary ball milling was performed to reduce the particle size to form a new powder. After the annealing treatment the material is consolidated and it was so hard that it resulted really difficult to make it powder again.

Fig. 9 shows the microstructure obtained for the powder after the annealing treatment. The microstructure resembles a nearly lamellar structure. The Young's modulus value obtained by nanoindenttation was 141 ± 27 GPa and the hardness obtained 4,7 ± 0,9 GPa, therefore, after annealing the hardness value is reduced compared to the initial state as it was desired, but the consolidation of the annealed form made this route difficult.

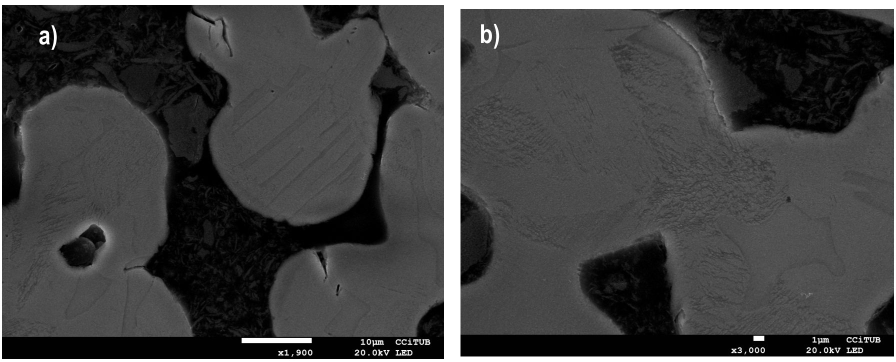

Fig.9: SEM micrographs of the treated powder at higher magnification

6.2. COLD GAS SPRAY COATINGS

The CGS coatings have been performed in the higher energy conditions as possible, with high pressure and temperature.

For a successful spraying of a metal onto metal substrate, it is necessary that whatever the spraying conditions are, there is a suitable metallurgical bonding between the two materials, this is that they show a capability to deform and disrupt any possible native oxide layer upon impact so that direct contact is promoted. For this to occur, usually particle velocities need to be within a window of deposition. Fig. 10 shows a macroscopic example given by 20 mm copper balls in homemade projectiles impacting onto a steel plate. Amount of explosives defined speed of the ball. Usually, the particles do not instantly adhere but rather there is a delay time. According to this figure, the results shown before for the splat morphologies, we would say that we are not well into the deposition window of the material.

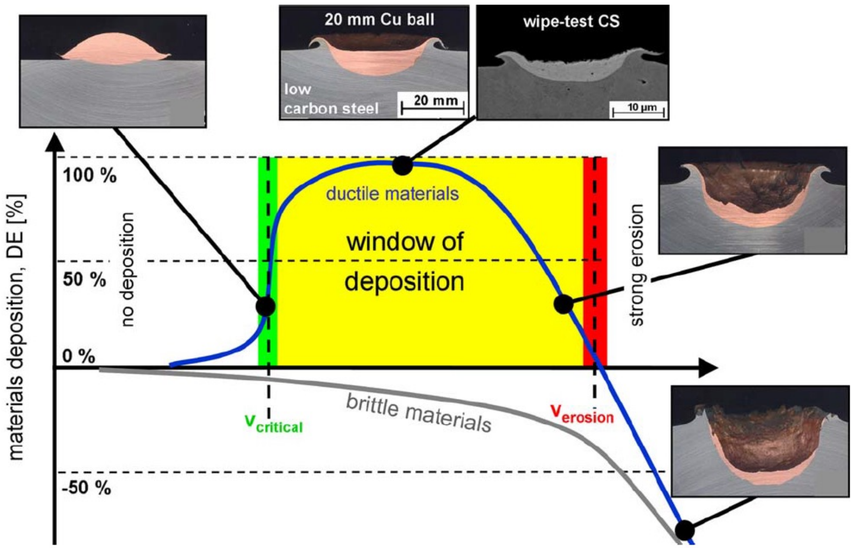

Fig 10. Schematic correlation between particle velocity, deposition efficiency (DE) and impact effects for a constant impact temperature. Deposition is only observed for ductile materials in a certain velocity range for a given powder size and temperature, the so-called ‘‘window of deposition’’.

6.2.1. TiAl (Ti48Al2Nb2Cr)

The results obtained in the powder characterization indicate that it will be difficult to build up a coating using this powder even if the more energetic conditions are used. Maybe when using an equipment with higher temperature and gas pressure, this would be more easily achieved; also, if helium rather than nitrogen would be used, it would allow to reach higher particle velocities. Fig. 11 shows an attempt to produce a coating. It is possible to observe how few particles adhere without existing uniformity in the coating. . The second layer of particles is not even produced; most of them may have bounced off when impacting onto the hard and stiff layer of the first bonded particles. Such second incoming particles do not finally bond and just produce further flattening of the adhered ones. Because of all this, the only use of the Ti-48Al-2Nb-2Cr powder is rule out to obtain the coating.

Fig. 11: One layer of Ti-48Al-2Nb-2Cr on Ti-6Al-4V.

6.2.2 TiAl + Al Composite

Due to some handicaps given by the low deformability of such powder alloy, it was decided to introduce the appropriate aluminium portion to obtain a composite coating aiming at achieving the $TiAl_3$ composition after an annealing treatment. The $TiAl_3$ can provide better high temperature resistance due to its higher Al content.

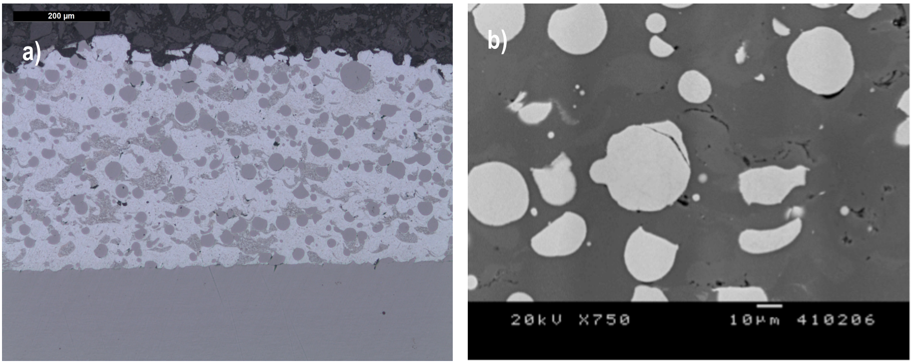

Fig. 12: (a) Optical micrograph of the as-sprayed CGS TiAl + Al composite coating onto Ti-6Al-4V substrate, (b) SEM micrograph of the coating at higher magnification.

The microstructure of the coating is shown in Fig. 12; the coating consist of highly deformed aluminium matrix with hardly distinguishable particle boundaries and relative undeformed TiAl particles embedded in the almost porosity free Al matrix. This can be explained by the fact that aluminium undergoes much more deformation than titanium aluminide due to its lower yield strength and much lower melting point. Also it is possible to observe uniformity in the distribution of the particles of TiAl in the coating. The coating-substrate is smooth because the substrate is not deformed by the impact of the soft aluminum particles.

The information obtained by the nanoindenter on the aluminium matrix is shown in Fig. 13. The values of Young's modulus obtained for the matrix of aluminium are: 80 ± 14 GPa. The value of hardness obtained are: 0,9 ± 0,3 GPa. The Young's modulus of aluminium with commercial purity has 70 GPa and the value of hardness 0,25 GPa. This increase of the hardness stems for the impact [19].

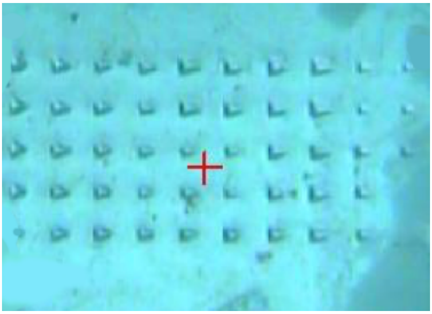

Fig. 13: Nanoindentions in aluminium matrix of CGS TiAl + Al composite coating.

Also the test is performed on the TiAl particles embedded in the aluminium matrix to observe the difference of the Young's modulus (Fig. 14). The Young's modulus obtained in the TiAl particles is 143 ± 36 GPa and the hardness for TiAl 6,5 ± 2,0 GPa, as presented in section 6.1.1.3. The hardness obtained for the Aluminium matrix in the surrounding of TiAl particles was found to be 1,2 ± 0,5 GPa, slightly higher than that previously presented

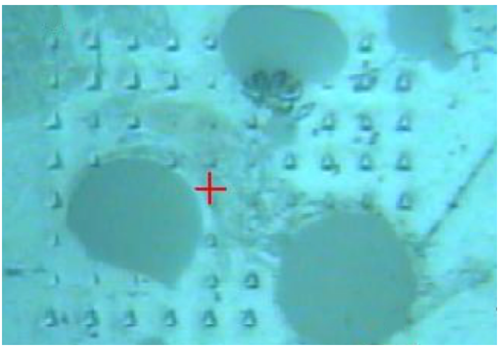

Fig 14: Nanoindentations in the CGS TiAl + Al composite coating.

6.2.2.1. Annealing treatments

The TiAl + Al composite CGS coatings were then exposed to different annealing treatments under Argon atmosphere in a tubular furnace in order to assess the formation of the $TiAl_3$ phase. All the samples were heated and cooled at an average rate of 3ºC/min.

The following treatments are based on some works found in the literature. Sienkiewicz et al. [20] performed annealing treatments at 600ºC to observe the increase of the porosity for TiAl. Novoselova et al. [5] performed different annealing tratments at 650ºC to obtain $TiAl_3$. Wang et al. [21] performed heat treatment for as-sprayed at 700ºC to form a pure $TiAl_3$ coating.

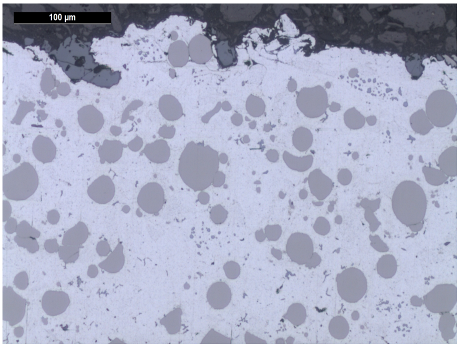

Fig. 15: Optical micrograph of the TiAl + Al coating after annealing treatment at 500ºC for 5h.

A cross-section image of the coating after the annealing treatment at 500ºC for 5 hours is shown in Fig. 15. In comparison with the non-treated coating, no changes in the microstructure are observed. The coating keeps the undeformed TiAl particles embedded in highly deformed aluminium matrix.

It was decided to increase the temperature of the annealing treatment to 600ºC with the aim to obtain $TiAl_3$. Representative cross-sectional images of the coating after the annealing treatment at 600ºC for 5 hours are shown in Fig.16.

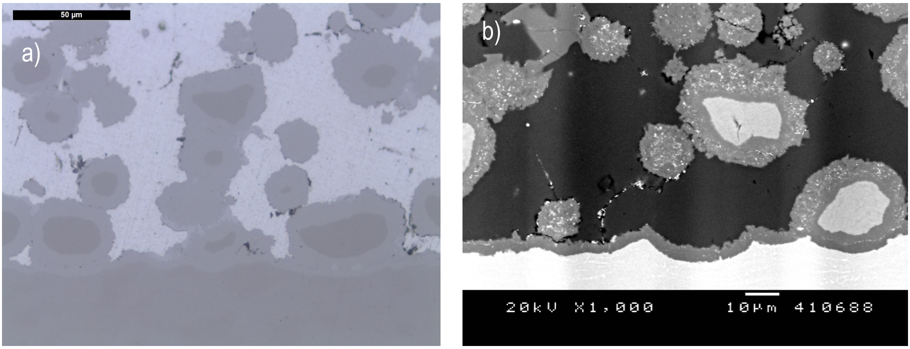

Fig. 16: (a) Optical micrograph of the TiAl + Al coating after annealing treatment at 600ºC for 5h. (b) SEM micrograph with the diffusion area much more visible.

The appearance of a diffusion layer is seen around the TiAl particles as well as the coating-substrate interface, however the particles keep the spherical structure. The SEM micrograph performed using backscattered electrons (BSE) shows very well the contrast of the different phases. In the BSE mode, the phases with higher atomic number are depicted with lighter grey contrast. In this case, the Ti6Al4V substrate is presented as very light and the diffusion layer shows a medium grey contrast compared to the dark aluminium matrix.

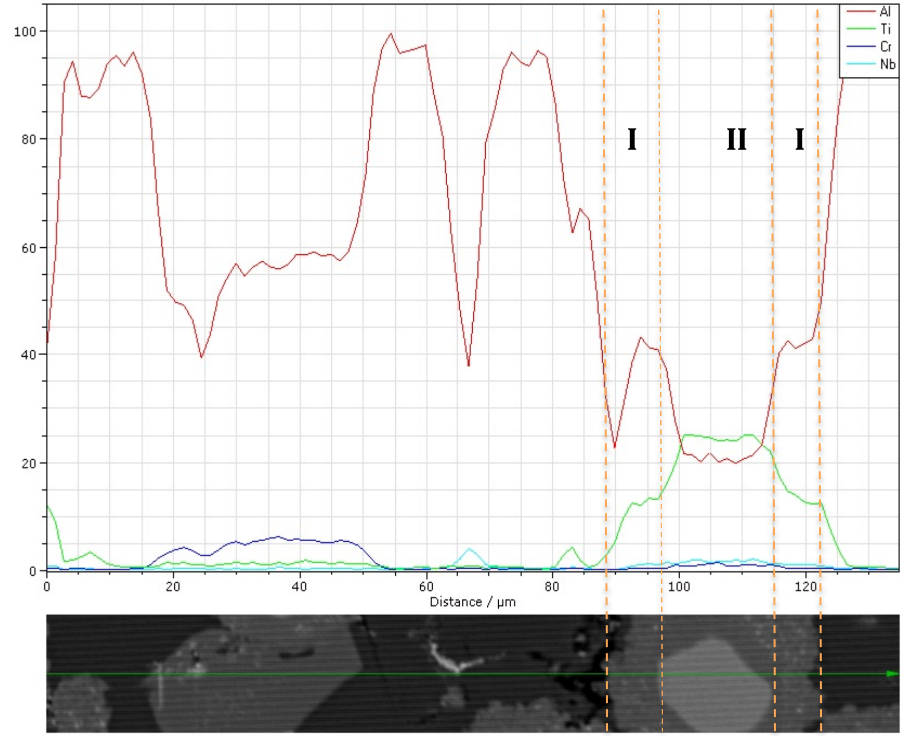

Fig. 17: EDS line profile analysis of TiAl + Al coating after annealing treatment at 600ºC for 5h.

The microanalysis by Energy Dispersive Spectra (EDS) in the SEM was used to determinate the composition of the different zones of the particles. Studies involving synthesis of titanium aluminides showed that $TiAl_3$ forms prior to the formation of any titanium aluminide because of the Gibbs free energy of this intermetallic phase, which is significantly lower than for other intermetallics [20]. As shown in Fig. 17 and calculated in Table 3, the zone I presents a similar composition to $TiAl_3$, the zone II, the lightest zone, presents the composition of the initial powder (Ti-48Al-2Nb-2Cr). This proves that the $TiAl_3$ intermetallic phases developed during the annealing treatment at 600ºC.

Element	Zone I at%	Zone II atomic %
Aluminium	72,55	46,22
Titanium	26,29	50,32
Niobium	0,73	1,7
Chromium	0,43	1,75

Table 3: Results of EDS line profile analysis for the coating annealed at 600ºC for 5 hours at zone I and zone II.

Fig. 18 shows the structure of the coating treated at 650ºC for 5 h [5]. Novoselova et al. [5] performed several annealing treatments for a cold-sprayed Ti+Al coatings and observed the formation of several titanium aluminide phases. Here, just two contrasts can be observed within the coating; the diffusion within the particles seems to be complete without remnants of the original TiAl composition. Due to the diffusion, some of the particles have coalesced. The compositional analysis shows that the diffused areas as mainly present the $TiAl_3$ based composition.

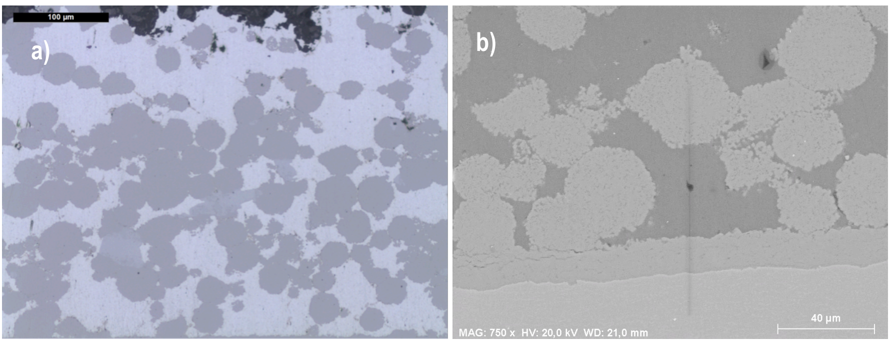

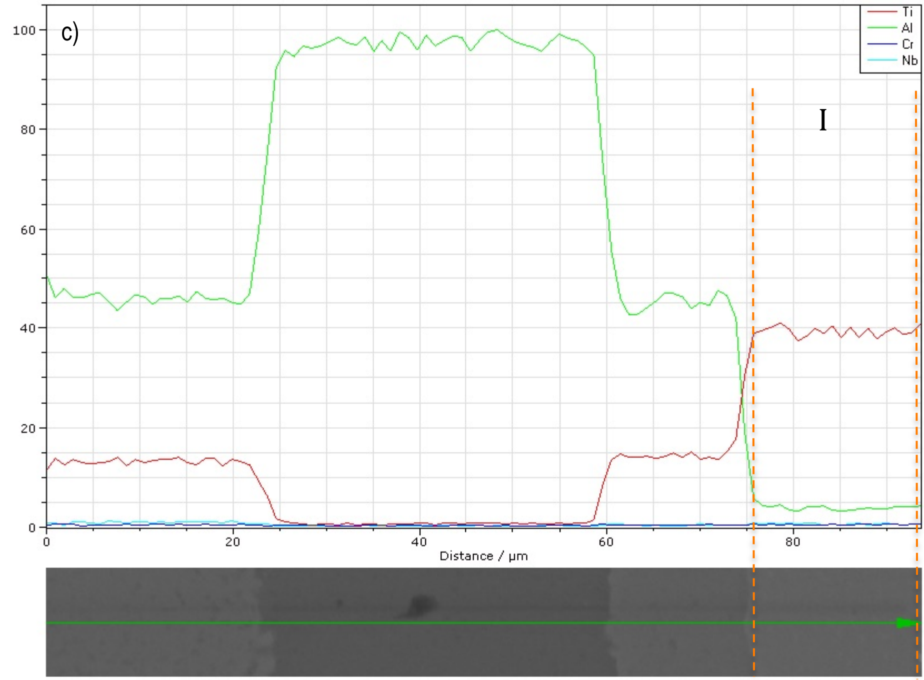

Fig. 18: (a) Optical micrograph of the TiAl + Al coating after annealing treatment at 650ºC for 5h, (b) SEM micrograph of the coating at higher magnification, (c) EDS line profile analysis of one region of the analysed coating.

Element	Zone I at%
Aluminium	71,00
Titanium	27,92
Niobium	0,44
Chromium	0,65

Table 4: Results of EDS line profile analysis for the coating annealed at 650ºC for 5 hours at zone I.

The samples treated at 700ºC are shown in Fig. 20. The micrographs prove that the proportion of each phase formed depend on the time at the annealing treatment. The sample treated at 700ºC for 10 min (Fig. 20 a) also shows the diffused areas around the TiAl particles, but in this case the diffusion becomes spread in a less uniform way, most probably because we are above the melting point of aluminium and the diffusion in the liquid phase takes place more rapidly. The samples treated for 1 and 1,5h (Fig. 20 b and c) show that the $TiAl_3$ phase became dominant as long as the aluminium phase was eliminated by diffusion into TiAl particles. Some unreacted aluminium still remained in the coating. Although the two samples present a good diffusion, the sample treated for 1,5h presents better uniformity of the $TiAl_3$ phase. The sample treated for 5h (Fig. 20 d) is formed by only one phase, $TiAl_3$. This means that diffusion between the substrate and the coating has taken place, but presents an elevated porosity and some cracks can be seen.

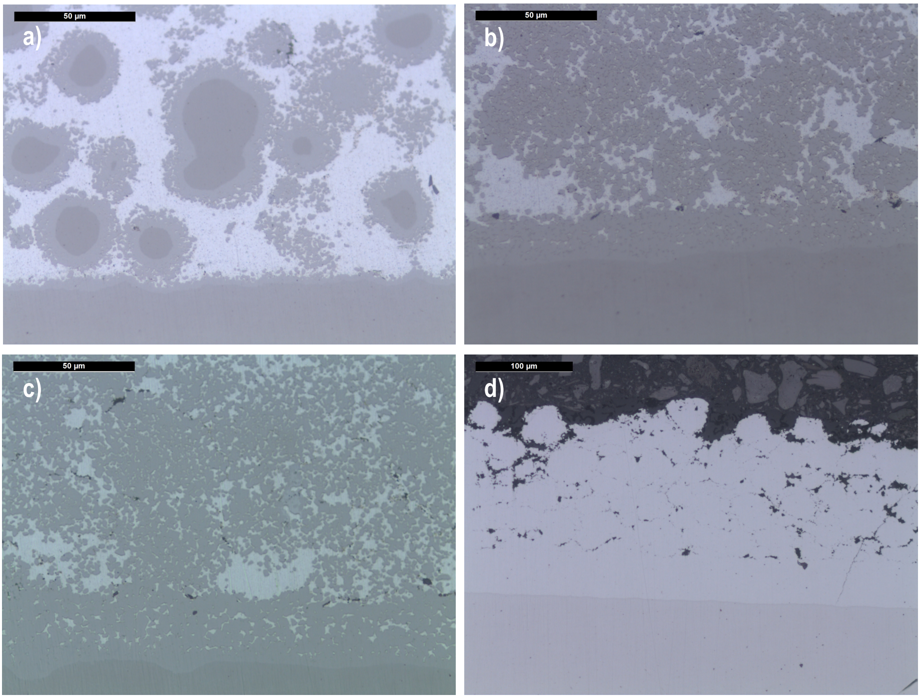

Fig. 20: Optical micrograph of the TiAl + Al coating after annealing treatment at 700ºC: (a) for 10 minutes, (b) for 1 hour, (c) for 1,5 hours, (d) for 5 hours.

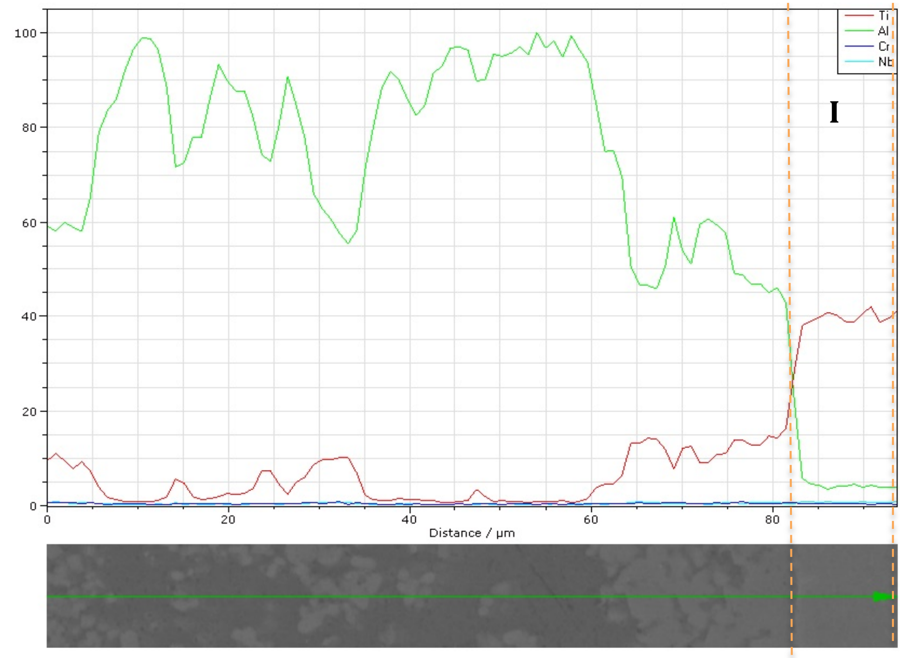

Fig. 21: SEM analysis of substrate with TiAl + Al composite coating after annealing treatment at 700ºC for 1 hour.

Element	Zone I atomic %
Aluminium	72,95
Titanium	25,86
Niobium	0,39
Chromium	0,80

Table 5: Results of EDS analysis for the coating subject to annealing treatment at 700ºC for 1 hour at Zone I.

As shown in Fig. 21 and calculated in Table 5, the analysis of a region within the coating treated at 700ºC for 1 hour shows, that the light contrast presents a composition of $TiAl_3$.

The information obtained by the nanoindenter on the treated coating at 700ºC for 1,5h is shown in Fig. 22. The values of Young's modulus obtained for the sample is: 157 ± 38 GPa. The hardness obtained for the coating treated is 4,6 ± 1,7 GPa.

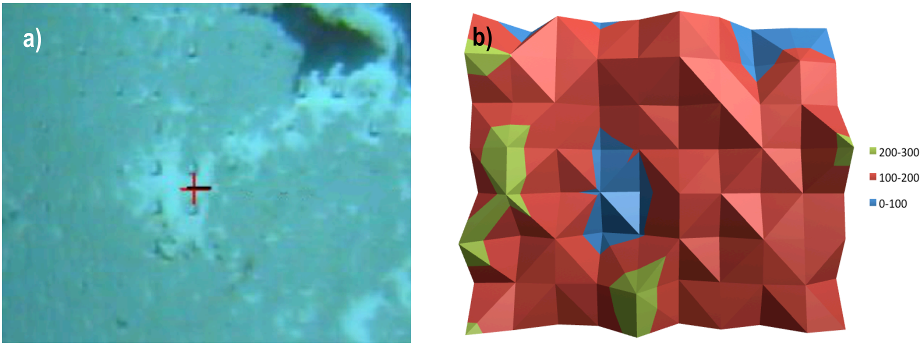

Fig 22: (a) Nanoindentater marks TiAl+Al composite after heat treatment at 700ºC for 1,5 (b) Representation of Young's modulus obtained in TiAl+Al composite after heat treatment at 700ºC for 1,5 h.

A very similar value of Young's Modulus is observed in the entire sample. It is possible to differentiate an area, in which the aluminium matrix keeps unaltered. This area can be observed in blue at fig. 22 b.

From all the above-presented treatments we decided the one at 700ºC for 1,5 hours in order to avoid porosity and try to get mostly the $TiAl_3$ phase.

6.2.2.2. Coating Oxidation

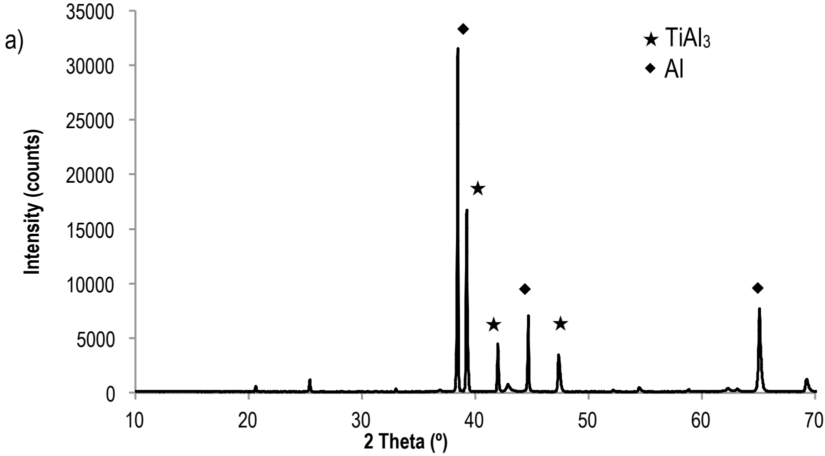

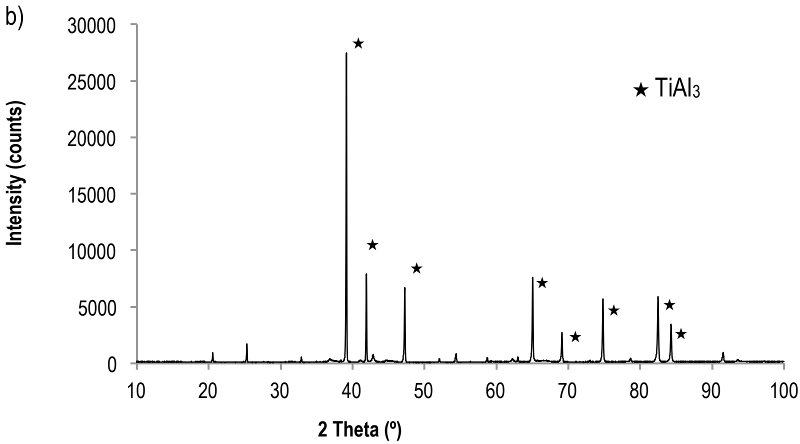

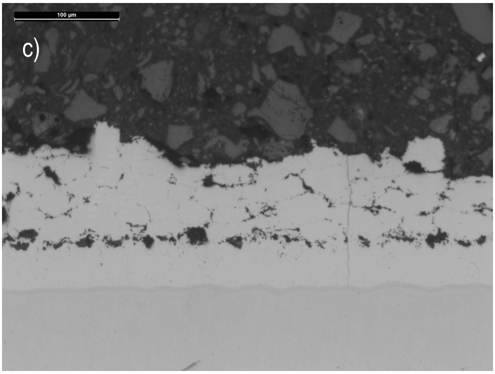

Fig 24: (a) XRD of the TiAl + Al coating after annealing treatment at 700ºC for 1,5h, (b) after isothermal oxidation test in Oxygen atmosphere at 750ºC (c) Optical micrograph of the TiAl + Al coating after annealing treatment at 700ºC for 1,5h and isothermal oxidation test in atmosphere of Oxygen at 750ºC.

Fig. 24 a shows the presence of the TiAl3 phase formed after the annealing treatment coexisiting with the remnant aluminum phase, whereas fig. 24 b, after the oxidation at 750ºC just presents the TiAl3 phase. Fig. 24 c shows the optical micrograph of the oxidized coating with the formation of some cracks, which indicates the fragility of the TiAl3 phase [16]; also some pores are observed due to the Kirkendall effect [5]. This is because of a large difference in the diffusivities of the diffusing species. In this system, where $TiAl_3$ is thought to grow by aluminium diffusing through the diffusion layer of $TiAl_3$ to form new intermetallic at the$TiAl_3$ /Ti coating-substrate interface and TiAl3/Al particle-matrix interface. There is a lack of diffusion coefficient data for Ti in Al. However, there are reports that the diffusivity of Al in Ti, TiAl, and $TiAl_3$ is faster than that of Ti.

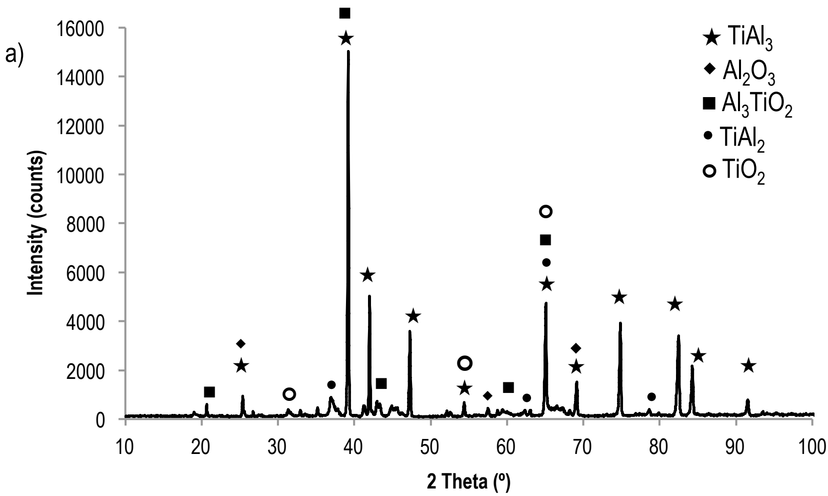

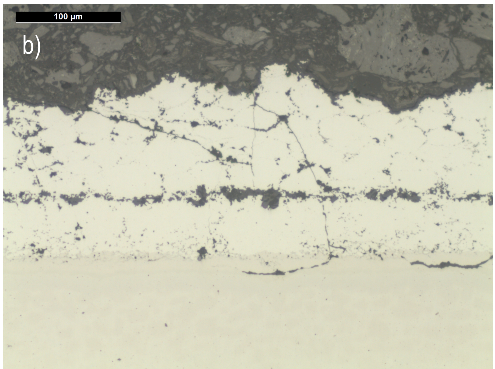

Fig 25: (a) XDR of the TiAl + Al coating after annealing treatment at 700ºC for 1,5h and isothermal oxidation test in atmosphere of Oxygen at 900ºC (b) Optical micrograph of the TiAl + Al coating after annealing treatment at 700ºC for 1,5h and isothermal oxidation test in atmosphere of Oxygen at 900ºC.

Fig 25 a shows the formation of different oxides: Al_2O_3, Al_3TiO_2 and TiO_2 formed during the oxidation treatment. In Fig. 25 b the formation few cracks of a major size than the oxidation at 750ºC is appreciated. Indicating a major formation of oxides, which crate stress in the structure creating some cracks. Also the void formation due to the Kirkendall effect is more significant, which may be a problem. This severe interdiffusion could be then harmful to the long-term oxidation resistance.

The protection provided by ternary trialuminide coatings obtained by Low Pressure Plasma Spray was also not absolute because a network of stress relief cracks formed in the coatings either during deposition or during the oxidation treatment. Stress relief cracking could be eliminated with the application of gradient coatings formed by incorporating varying amounts of substrate powder in the first spray layers [12].

6.2.2.3. Dry sliding wear test

The wear performance was evaluated for the original Ti6Al4V substrate and compared with the as-sprayed TiAl+Al and annealed coatings.

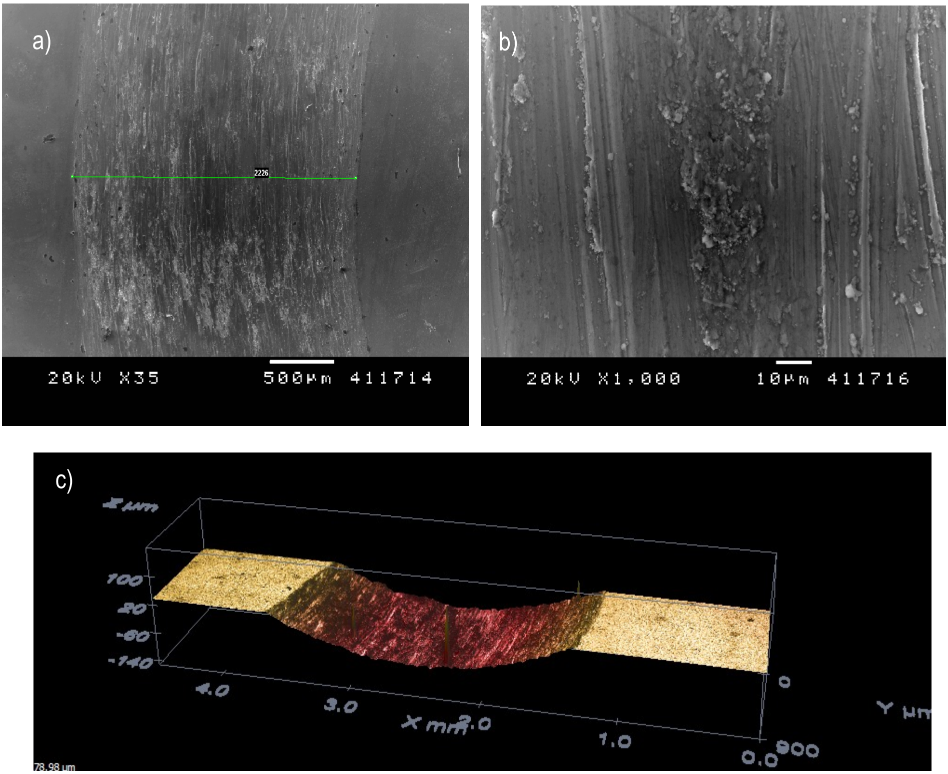

Fig. 27: (a) and (b) wear track SEM morphologies of the cross section of the substrate after the sliding test, (c) 3D representation of the wear track.

The wear track features of the substrate Ti-6Al-4V are shown in fig. 26. The general view is illustrated in fig. 26 a, while the morphological features are observed in fig. 26 b. Here scratch wear scars with some fractured regions indicate an abrasive mechanism. The mechanism of abrasion can be explained based on the fact that the tungsten carbide ball has considerably higher hardness than titanium samples [22]; also the wear debris remains between the two surfaces producing a third-body abrasion effect. Fig. 26 c shows the 3D profile of the wear track obtain by confocal microscopy. The maximum depth of the wear track is 100 μm and the width is 2150 μm.

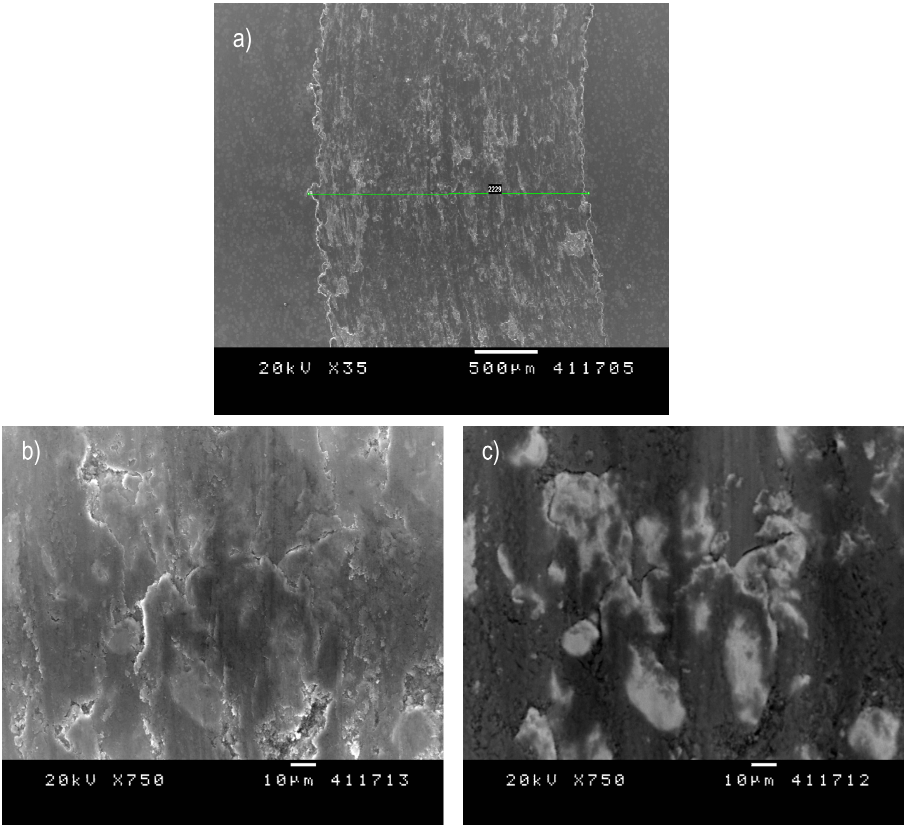

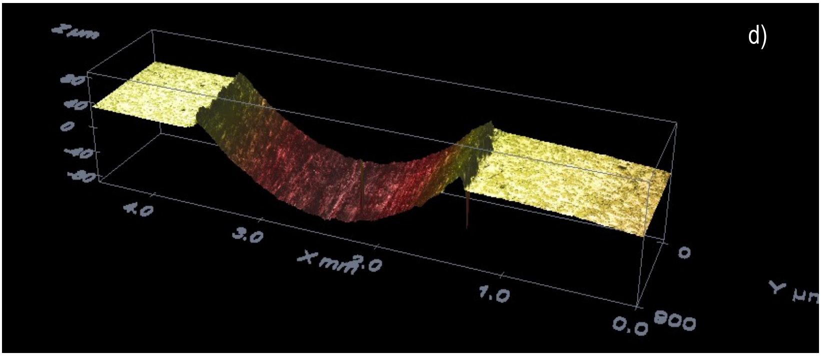

Fig. 27: (a),(b) and (c) wear track SEM morphologies of the cross section of the CGS TiAl + Al coating after the sliding test, (d) 3D representation of the wear track.

The wear track morphologies of TiAl+Al composite coating are shown in fig. 27. At high magnification (fig. 27 b) the wear mechanism is revealed to be adhesive with the typical smeared appearance.

Fig. 27 c shows the same region of fig. 27 b but in the BSE mode, some interconnected cracks can be observed. Fig. 27 d shows the 3D profile of the wear track; the maximum depth was 92 µm and the width was 2200 µm.

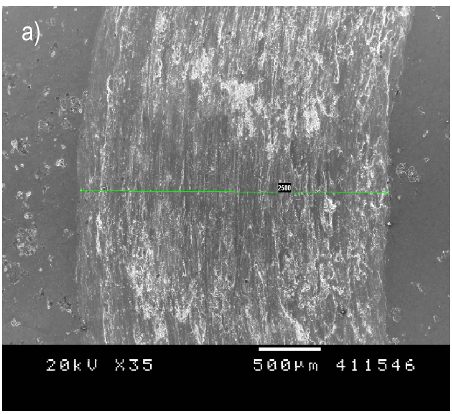

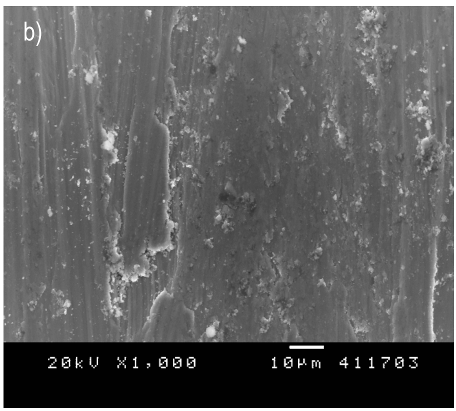

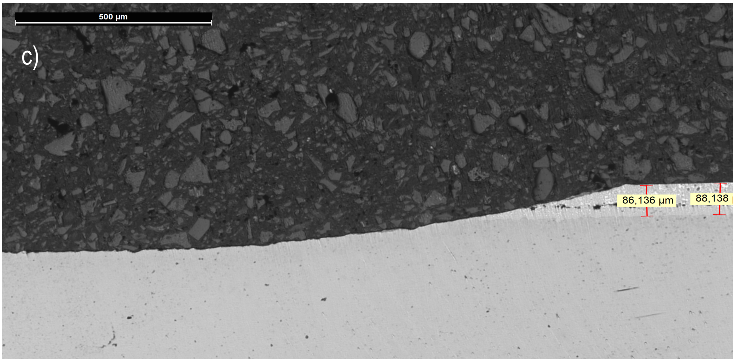

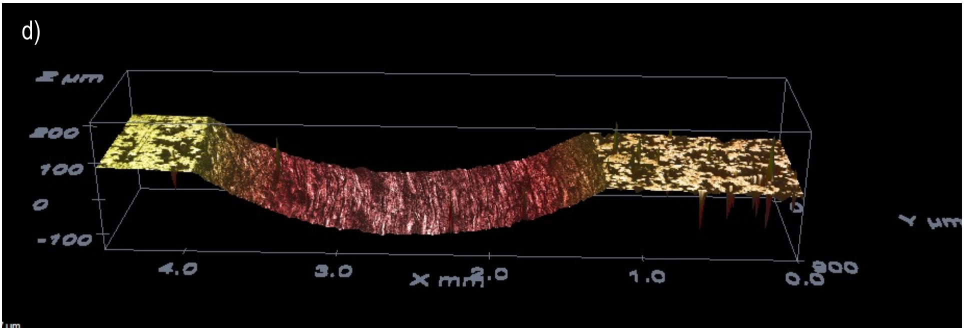

Fig. 28: (a) and (b) wear track SEM morphologies and (c) optical micrograph of the cross section of the CGS TiAl + Al coating after annealing treatment at 700ºC for 1,5 hours after the sliding test. (d) 3D representation of the wear track.

The wear track morphologies of TiAl+Al composite coating after annealing treatment at 700ºC for 1,5 hours are shown in fig. 28. At high magnification (fig. 28 b) the wear mechanism is revealed to be mainly abrasive mechanism.

Fig. 28 c shows as the wear test arrives to the substrate causing wear in the substrate. Fig. 28 d shows the 3D profile of the wear track; the maximum depth obtained was 152 µm and the width was 2500 µm.

The coefficient of friction, the depth and width are higher than the expected initially. A distinction is often made between two-body and three-body abrasive wear, where the latter refers to situations in which hard particles are introduced between the moving surfaces [23]. In this case the abrasion takes place initially in the coating and later in the substrate, is possible that some coating particles remaining between the ball and the substrate acting like a three body increase the abrasive wear in the substrate.

	Wear rate (mm^3/Nm)	Maximum depth (µm)	Width (µm)
Substrate	$6{,}78 \cdot 10^{-4} \pm 3{,}39 \cdot 10^{\wedge-5}$	100	2150
As-sprayed	$7{,}33 \cdot 10^{-4} \pm 1{,}22 \cdot 10^{-5}$	92	2200
Ar 700ºC 1,5h	$1{,}32 \cdot 10^{-3} \pm 5{,}36 \cdot 10^{-5}$	152	2500

Table 6: Comparison of the different values obtained.

Table 6 shows the values of the wear rate indicating that the as-sprayed samples have the highest resistance.

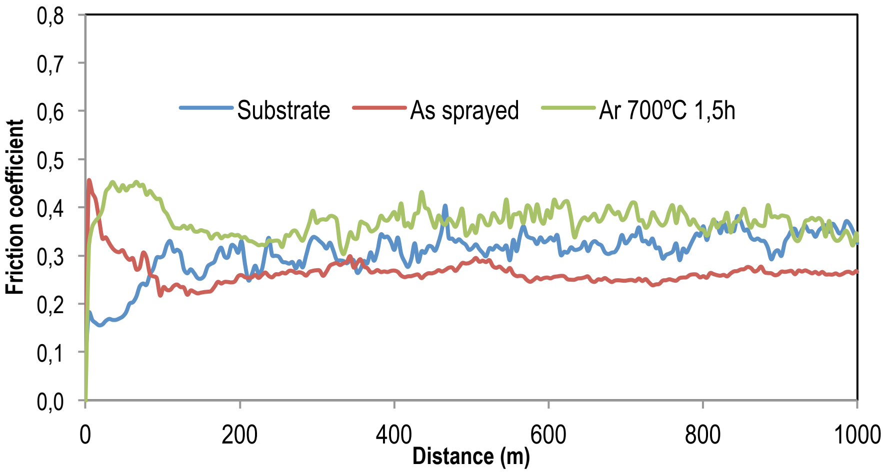

Fig. 29: Evolution of friction coeficient for three tested samples.

Fig. 29 shows the evolution of friction coefficient for the three tested samples. It can be seen that the lowest values corresponds to the as-sprayed coating, while the samples showing and abrasive behavior exhibit a higher coefficient. The annealed sample shows a drop after the first 100 meters; this is may correspond to the starting of the wear of the substrate.

7. CONCLUSIONS

After this work has been completed, the following conclusions have been extracted:

- Titanium trialuminide coatings were produced by Cold Gas Spray. The build up of and entire TiAl coating was difficult because of the low deformation capability of the raw material.
- TiAl+Al composite coatings were successfully produced with a uniform distribution of the titanium aluminide particles with in aluminium matrix. The as-sprayed aluminium became hardened because of the impact.
- The annealing treatment in argon atmosphere at 700ºC for 1,5h was selected has optimum for the obtaining of a titanium trialuminide coating without void and cracking. The exposure at higher temperatures and longer times resulted in the formation of voids due to the Kinkerdall effect.
- The oxidation treatment at 750ºC for 24 hours resulted in the fully formation of the titanium trialuminide phase, which was observed to be very brittle. At 900ºC for 24 hours the formation Al_2O_3 also with some TiO_2 was observed. The coating failure may be more provably given by the brittleness of $TiAl_3$ phase rather than the accelerated oxidation of the TiO_2.
- The as-sprayed TiAl+Al coating showed an adhesive mechanism while the substrate and the annealed coating showed mainly an abrasive mechanism. The highest wear resistance (lowest wear rate) corresponded to the as-sprayed composite coating.

8. REFERENCES AND NOTES

1. S. Winstein, In *University Chemical Education,* Proceedings of the International Symposium on University Chemical Education, Frascati (Rome), Italy, 1969; Chisman, D. G.. Ed.; Butterworths: London, 1970.
2. M.Yamaguchi, H.inui, K.Ito; High-temperature structural intermetalics, Acta mater.; 2000: 48: 307-322.
3. Intermetallic materials, Intermetallic materials for structural high temperature applications Ref p. 14-38.
4. http://metal2012.tanger.cz/files/proceedings/metal_09/Lists/Papers/077.pdf
5. T. Novoselova, S. Celotto, R. Morgan, P.Fox, W. O'Neil; Formation of TiAl intermetalics by heat treatment of cold-sprayed precursor deposits, Journal of Alloys and Compounds; 2007: 436: 69-77.
6. D. Vojtêc, T. Kubatík, M. Pavlícková, J. Maixner, Intermetallic protective coatings on titanium. Intermetalics; 2006: 14: 1181-1186.
7. Z. Liu, G.Wang, Improvement of oxidation resistance of γ -TiAl Al 800 and 900 ºC in air by $TiAl_2$ coatings. Materials Science and Engineering A; 2005: 397: 50-57.
8. Gross K.Thermal spraying- an introduction, http://www.azom.com/Details.asp?ArticleID=542.
9. H. Gyo Jung, K. Young Kim Effect of Ternary Elements of the Oxidation Behavior of Aluminized TiAl Alloys, Oxidation of materials; 2002: 58: 197-216.
10. N.Cinca, J.M.Guilemany Thermal spraying of transition metal aluminides: An overview, Intermetalics: 2012: 24: 60-72.
11. F.Gärtner, T.Stoltenhoff, T.Schmidt, Journal of Thermal Spray Technology, 2006:15: Issue 3.
12. M. Villa, Metallic coatings deposited by Cold Gas Spray onto light alloys, Doctoral Thesis; 2013
13. Y.W.Kim, Journal of Metals 1994: 46: 30-40.
14. https://xos.com/technologies/xrd/
15. http://www.microscopy.ethz.ch/bragg.htm
16. G.E.Fuchs, The efect of Processing on the Hot Workability of Ti-48Al-2Nb-2Cr Alloys, Metallurgical and materials transactions; 1997: 28A: 2543-2553.
17. T. Schmidt; H. Assadi; F. Gärtner; H. Richter; T. Stoltenhoff; H. Kreye, T. Klassen; Journal of Thermal Spray Technology, 2009: 18: Issue 5; 794-808 [Revista Peer Reviewed].
18. http://www.erasteel.com/content/gas-atomization-0
19. CES EduPack 2016
20. J. Sienkiewicz, S. Kuroda, R. M. Molak, H. Murakami, H. Araki, S. Takamori, K. J. Kursydlowski, Fabrication of TiAl intermetallic phases by heat treatment of warm sprayed metal precursors; Intermetallics; 2014: 49, 57-64.
21. J. Wang, L. Kong, T. Li, T. Xiong, Oxidation behavior of thermal barrier coatings with a $TiAl_3$ bond coat on γ-TiAl alloy, Journal of Thermal Spray Technology; 2015: 24: Issue 3: 467-473.
22. C.X. Li, J.Xia, H. Dong; Sliding wear of TiAl intermetallics aganist Steel and ceramics of Al_2O_3, Si_3N_4 and WC/Co, Sience Direct; 2006: Wear 261: 693-701.
23. K. Holmberg, A. Matthews; Coatings tribology; properties, techniques and Applications in surface engineering; Elsevier; 1994: Tribology series 28: 45-55